A spatio-temporal analysis of the environmental correlates of COVID-19 incidence in Spain

Antonio Paez[*,a], Fernando A. Lopez[b], Tatiane Menezes[c], Renata Cavalcanti[d], Maira Galdino da Rocha Pitta[d]

[a]*School of Geography and Earth Sciences, McMaster University, 1281 Main St W, Hamilton, ON, L8S 4K1, Canada*
[b]*Departamento de Metodos Cuantitativos, Ciencias Juridicas, y Lenguas Modernas, Universidad Politecnica de Cartagena, Calle Real Numero 3, 30201, Cartagena, Murcia, Spain*
[c]*Departamento de Economia, Universidade Federal de Pernambuco, Av dos Economistas, s/n - Cidade Universitária, Recife - PE, 50670-901, Brasil*
[d]*Núcleo de Pesquisa em Inovação Terapêutica NUPIT / UFPE, Av. Prof. Moraes Rego, 1235 - Cidade Universitária, Recife, PE, CEP 50670-901, Brazil*

Abstract

Spreading with astonishing speed, the novel SARS-CoV2 has swept the globe, causing enormous stress to health systems and prompting social distance guidelines and mandates to arrest its progress. While there is encouraging evidence that early public health interventions have slowed the spread of the virus, this has come at a high cost as the global economy is brought to its knees. How and when to ease restrictions to movement hinges in part on the question whether SARS-CoV2 will display seasonality associated with variations in temperature, humidity, and hours of sunshine. In this research, we address this question by means of a spatial analysis of the incidence of COVID-19 in the provinces in Spain. Use of a spatial Seemingly Unrelated Regressions (SUR) approach allows us to model the incidence of reported cases of the disease per 100,000 population, as a function of temperature and humidity, while controlling for GDP per capita, population density, percentage of older adults in the population, and presence of mass transit systems. An interesting aspect of the spatial SUR approach is that it models incidence as a contagion process. Our results indicate that incidence of the disease is lower at higher temperatures and higher levels of humidity, although coefficients for this variable are significant only in some equations. Sunshine, in contrast, displays a positive association with incidence of the disease. Our control variables also yield interesting insights. Higher incidence is associated with higher GDP per capita and presence of mass transit systems in the province; in contrast, population density and percentage of older adults display negative associations with incidence of COVID-19.

[*]Corresponding Author
Email addresses: paezha@mcmaster.ca (Antonio Paez), fernando.lopez@upct.es (Fernando A. Lopez), tatiane.menezes@ufpe.br (Tatiane Menezes), renata.vcsantos@gmail.com (Renata Cavalcanti), mgrpitta@ufpe.br (Maira Galdino da Rocha Pitta)

Introduction

From a small outbreak linked to a live animal market at the end of 2019 to a global pandemic in a matter of weeks, the SARS-CoV2 virus has threatened to overrun health systems the world over. In efforts to contain the spread, numerous governments in many nations and regions have either recommended or mandated social distancing measures, and as of this writing, millions of people in five continents shelter in place. There are encouraging signs that these measures have arrested the spread of the virus where they have been implemented, and have thus helped to keep a bad situation from becoming even worse (e.g., 2020). However, this has come at a high cost, and the consequences for all spheres of the economy, social, and cultural life have been dire (e.g., Fernandes, 2020; Luo and Tsang, 2020). As a result, there is a sense of urgency to anticipate the progression of the pandemic, in order to plan for progressive lifting of restrictions to movement and social contact (e.g., Kissler et al., 2020). Needless to say, this has become a delicate, and politically charged, balancing act between public health and the economy (Gong et al., 2020).

A salient question in the debate on how and when to ease social distancing measures is whether the virus will display seasonal variations. Earlier, diverse studies have shown the effect of temperature and humidity on the incidence of influenza (e.g., Mäkainen et al., 2009; Jaakkola et al., 2014; Kudo et al., 2019). Jaakkola et al. (2014), for example, found that a decrease of temperature and absolute humidity precedes the onset of symptoms of influenza A and B viruses by 3 days in places where the temperature is low. After the 2002-2004 outbreak of SARS, researchers also began to investigate the relationship between these factors and SARS-CoV. In this way, Casanova et al. (2010) used two surrogates, namely the gastroenteritis (TGEV) and mouse hepatitis viruses (MHV), to find that virus inactivation was more rapid at temperatures of 20C than 4C, and at 40C than 20C; in terms of humidity, these researchers reported that survival of the virus was lower at moderate relative humidity levels. In a similar vein, but working directly with SARS-CoV, Chan et al. (2011) found that viability of the virus was lost at temperatures higher than 38C and relative humidity superior to 95%.

While existing research on similar pathogens suggests that SARS-CoV is more stable and potentially easier to transmit in conditions of low temperature and low humidity, it is far from certain that this will also be the case with the novel SARS-CoV2. If such is the case, there is the possibility of easing restrictions to social contact as the weather warms; however, weeks or possibly months of costly measures could become undone if not, and the restrictions are lifted prematurely. Not surprisingly, given the stakes involved, this issue has already triggered a lively debate.

Some of what is thought about the possible seasonality of COVID-19 is based on analogies to the patterns of other known respiratory viruses. However, de Ángel Solá et al. (2020) note that "not all seasonal respiratory viruses experience the same spatiotemporal patterns" (section 4). This urges caution when extrapolating from known viruses, and indeed, the evidence in this respect

is inconclusive. At a global scale, de Ángel Solá et al. (2020) see less risk in the Caribean Basin; however, Coelho et al. (Coelho et al., 2020) warn that at least during the exponential phase, expansion of the virus is not driven by climate. Similarly, whereas Araujo and Naimi (2020) argue that spread of SARS-CoV2 will likely be constrained by climate, Harbert et al. (2020) remain unconvinced that spatial modelling can currently discriminate the distribution of the disease on the basis of climate, at least in the United States. Yao et al. (2020), examined data from China and came to the conclusion that neither temperature nor ultraviolet indices had an association with transmission of COVID-19. This is despite previous research that has linked less exposure to UVB radiation to higher prevalence and severity of acute respiratory tract infections (Zittermann et al. 2016; Dąbrowska-Leonik et al. 2018; Dinlen et al. 2016; Mathyssen et al. 2017; Esposito and Lelii 2015; Jat 2017; Moriyama, Hugentobler, and Iwasaki 2020). To further complicate matters, much of the relevant work has yet to be peer-reviewed and therefore is open to change (see for example the challenge of Harbert et al. (2020) to Araujo and Naimi (2020)). In the United States, the National Academy of Sciences, Engineering, and Medicine was engaged by the Office of the Executive for guidance on this matter (see National Academies of Sciences, Engineering and Medicine, 2020). Their conclusion summarizes the situation well (see p. 6): "Some limited data support a potential waning of cases in warmer and more humid seasons, yet none are without major limitations... Additional studies as the SARS-CoV-2 pandemic unfolds could shed more light on the effects of climate on transmission."

With the above considerations in mind, our objective with this paper is to contribute to the knowledge basis regarding the spread of COVID-19 and the influence of environmental factors, particularly temperature, humidity, and sunshine. We adopt a population health approach, and report results from a spatial model of the incidence of COVID-19 in fifty provinces in Spain, one of the countries hardest hit by the pandemic. We combine data on reported cases of the disease with metereological information, to create a spatio-temporal dataset covering a period of 30 days. We then join this dataset with provincial-level economic and demographic information to act as controls to our key environmental variables. These data are analyzed using a spatial Seemingly Unrelated Regressions (SUR) approach, which allows us to model incidence of COVID-19 as a spatial contagion process.

The results provide evidence of the effect of temperature, humidity, and sunshine on the incidence of COVID-19. The clearest result with respect to these variables is a lower incidence of COVID-19 at higher temperatures and levels of humidity, while the opposite happens with respect to hours of sunshine. Our control variables also provide some intriguing insights. Higher incidence is associated with higher GDP per capita and presence of mass transit systems in the province; in contrast, population density and percentage of older adults display negative associations with incidence of COVID-19. The results of this analysis provide support to the hypothesis of seasonality of the novel SARS-CoV2, and should be of interest to public health officials and policy makers grappling with the question of the trajectory of the pandemic.

Please note that this paper is prepared as a reproducible research document. The source R Markdown document, as well as all data and code needed to reproduce/review/extend the analysis can be obtained from the following repository:

https://github.com/paezha/covid19-environmental-correlates/tree/master/Environmental-Correlates-of-COVID19-Spain

Context and Data

Covid-19 in Spain

The first reported case of COVID-19 in Spain was on January 31th, when a German tourist in the Canary Islands tested positive for the virus. However, it was still a few weeks before the first domestic case was reported, on February 27th in Sevilla province (Andalusia). In a short period of time, after this relatively slow start, the outbreak flared. By March 11th the World Health Organization (WHO) declared COVID-19 officially a pandemic. This declaration marked a turning point for the public in Spain too. As of March 13th, the number of cases of COVID-19 reported in Spain was 4,473, with a majority of cases (1,990) concentrated in Madrid: these numbers were at the time the worst outbreak in Europe, after Italy. In response to the situation, on March 13th the Spanish National Government declared a state of emergency, to go into effect on Saturday March 14th. As part of the state of emergency restrictions to most activities were imposed, with the exception of essential services (e.g. food, health) and some economic subsectors of industry and construction. A few days later, on March 17th, Spain closed its lands borders to allow entry only to returnee nationals and permanent residents. The lockdown was further hardened between March 30th and April 12th (including the Easter weekend of April 10th-12th) and during this period only essential activities were allowed. During this period, there was a dramatic reduction in overall mobility, both within provinces as between [1].

Selection of Variables

The global emergence of infectious diseases is mostly driven by environmental, ecological, and socio-economic factors (Jones et al., 2008). In the case of SARS-CoV2, the ecological factors include the interaction between humans and wildlife. Once transmission of a disease begins to happen between humans, socio-economic and environmental factors become increasingly important. As noted in the introduction, the focus of the paper is on environmental variables, namely temperature, humidity, and sunshine. These variables have been implicated in the viability and ease of transmission of similar viruses. In addition to these variables, we also aim to use a set of controls, in the form of specific socio-economic and demographic characteristics of each province.

[1] https://www.mitma.gob.es/ministerio/covid-19/evolucion-movilidad-big-data/movilidad-provincial

The first variable that we consider is GDP per capita. Much has been said about globalization and the spread of infectious disease[2]. The growth in global connections has presented a challenge to spatial approaches in the initial stages of disease management, when the cause of a disease may still be unclear, but the plane has already departed (Zhou and Coleman, 2016). In reference to the earlier outbreak of SARS, van Wagner (Van Wagner, 2008) chronicles how Toronto's status as a global city turned out to be a vulnerability in this respect. In our case, we think of GDP per capita as a marker of a region's relative position in a network of global cities, and its potential to be further ahead in the trajectory of the pandemic. Furthermore, wealthier regions also tend to concentrate more activities that produce non-traded goods, including building and construction (Hallet, 2002). Therefore, it is possible that wealthier regions remain relatively more active even during a lockdown. On the other hand, it is also possible that less wealthy regions have a higher proportion of workers in manual occupations that cannot telework, and therefore have more difficulties complying with shelter-in-place orders.

The percentaje of older adults (over 65) is the second variable that we consider as a control. Early evidence regarding COVID-19 suggests that the case rate mortality is higher at older ages (e.g. The Novel Coronavirus Pneumonia Emergency Response Epidemiology Team, 2020). However, it is not clear that a relatively large population of older adults necessarily translates into higher transmission of the infection. The tool of choice in containing the spread of the disease has been social distancing. In this respect, the evidence from the field of transportation is that older adults tend to travel less frequently, for shorter distances, and have higher rates of immobility (e.g., Roorda et al., 2010; Morency et al., 2011; Sikder and Pinjari, 2012). In other words, many older adults are, whether by preference or otherwise, already in a form of social isolation. Social distancing during the pandemic may actually reinforce that condition for them, as suggested by the analysis of age-structured social contact in India, China, and Italy of Sing and Adhikari (2020). Accordingly, our expectation is that provinces with higher percentages of older adults will tend to have similarly low levels of social contact, particularly since the age-structured matrix of social contact in Spain is similar to Italy (Prem et al., 2017).

The third population variable the we consider is population density, since it directly affects the contact patterns and contact rates between individuals in a population (Hu et al., 2013). The evidence available suggests a positive relationship between the transmission of COVID-19 and population density (e.g. cumulative incidence in urban areas like NYC). For this reason, we anticipate a positive relationship between population density and the incidence of the disease.

The last control variable is the presence of mass transit systems in a province.

[2]As the Globe and Mail, Canada's paper of record, put it in relation to the SARS outbreak in 2003: "Globalization means that if someone in China sneezes, someone in Toronto may one day catch a cold" (Editorial, March 28, 2003, p. A18)

Every province in Spain offers some form of public transportation, however only five provinces have higher order systems of mass mobility (e.g. metro or subway), namely Barcelona, Madrid, Sevilla, Valencia, and Bizkaia. Public transportation has been hypothesized to relate to the spread of contagious disease by some researchers using agent-based approaches and simulation (e.g., Perez and Dragicevic, 2009; Wang et al., 2010), and while we find scant evidence of a link in the literature, the idea is intuitively appealing. After all, unlike the isolation that a car offers to travellers, most mass transit system are cauldrons of social contact.

Data

Our dataset includes information about the daily number of cases of COVID-19 reported in Spain at the provincial level (NUTIII in Eurostat terminology) for the period between March 13th and April 11th, inclusive. For our purposes, we consider positive cases reported, but excluding symptomatic cases diagnosed by a doctor without a Polymerase Chain Reaction (PCR) test. The Spanish National Government publishes periodic updates at the regional level (NUTII) and the information is also released at the provincial level as part of a collaborative project by geovoluntarios.com[3], ProvidencialData19[4], and ESRI España. This information is compiled from several sources, mainly the official web pages of the Spanish regional goverments, as documented in Centro de Datos Covid-19[5]. In addition, we consider two sets of explanatory variables. The first one, and the focus of this research, is set of two environmental variables, namely temperature and humidity, which are collected from official sources (i.e., *AEMET*, the state meteorology agency, and *MAPA*, the ministry of agriculture, fisheries, and food). The second set provides some relevant controls for multivariate analysis, and refers to economic and demographic attributes of the province (also collected from official sources, i.e., INE, the national statistics institute). Table 1 shows the descriptive statistics and the provenance of the data.

The spatial and temporal coverage of the data is as follows. Our dataset begins on March 13, which is the first date when every province had reported at least one case of COVID-19, and continues until April 11, for a period of 30 days. The unit of analysis is the province. Provinces are the equivalent of states, and are embedded in Autonomous Communities. As an example, Cataluña is an Autonomous Community and consists of four provinces, namely Barcelona, Gerona, Lerida, and Tarragona. The size of the provinces is relatively large, as seen in Table 1. The smallest province is $1,978.12 km^2$ (this is smaller than Rhode Island in the US) and the largest province is $21,767.93 km^2$ (slightly smaller than New Jersey in the US). While this is a relatively large degree of spatial aggregation, reporting on COVID-19 is inconsistent at smaller geographies, or

[3]https://www.geovoluntarios.org/
[4]https://www.datoscovid.es/pages/providencialdata19
[5]https://www.datoscovid.es/pages/sobre-la-iniciativa

Table 1: Descriptive statistics

Variable	Note	Min	Mean	Max	SD	Source
COVID-19 Incidence	Incidence in reported cases of SARS-19 per 100,000 people	0.38	153.61	1149.36	186.23	ProvidencialData19
Area	Area of province in sq.km	1978.12	10118.79	21767.93	4.77	INE
GDPpc	GDP per capita in €1,000s	16.67	22.51	36.00	4805.98	INE
Older	Percentage of people aged 65 and older in the province	15.16	21.03	31.36	3.95	INE
Population Density	Population density in the province in people per sq.km	8.60	140.04	829.76	181.25	INE
Mean Temperature	Mean temperature in province by date, in C	1.00	12.18	23.20	3.67	AEMET
Humidity	Relative humidity in province by date	2.00	77.82	100.00	10.37	MAPA

Note:
ProvidencialData19: https://www.datoscovid.es/pages/providencialdata19
INE (Instituto Nacional de Estadistica): https://www.ine.es/
AEMET (Agencia Estatal de Meteorologia): http://eportal.mapa.gob.es
MAPA (Ministerio de Agricultura, Pesca y Alimentacion): http://eportal.mapa.gob.es

cases are not reported at that level at all. The analysis must therefore be considered ecological.

An important aspect of working with environmental data such as temperature and humidity is the incubation period of the disease. Lauer et al. (2020) report for the case of COVID-19 a median incubation period of 5.7 days (with a confidence interval between 4.9 to 7.8 days). The vast majority of cases (95%) develop symptoms between 2.6 days (CI, 2.1 to 3.7 days) and 12.5 days (CI, 8.2 to 17.7 days). For this reason, we judge it best to use lagged values of the environmental variables. We test different time lags as follows. We consider a lagged 8-day average, from date-minus-12 to date-minus-5 days (hereafter *lag8*). Secondly, we consider a lagged 11-day average, from date-minus-12 to date-minus-2 days (hereafter *lag11*). Finally, to account for the likely duration of incubation, we consider a lagged 11-day *weighted* average, from date-minus-12 to date-minus-2 days (hereafter *lag11w*). The weights for this variable are calculated using the parameters of the log-normal distribution reported by Lauer et al. (2020), i.e., a log-mean of 1.621 and a log-standard deviation of 0.418. With these weights, the environmental variables at date-minus-2 and date-minus-12 days are weighted as 0.041 and 0.009 respectively, whereas the environmental variables at date-minus-5 days are weighted as 0.194.

Methods: the Spatial SUR Model

The Seemingly Unrelated Regression equations model (SUR hereafter) is a multivariate econometric model used in different fields when the structure of the data consisits of cross-sections for different time periods. The basis of this approach is well-known since the initial works of Zellner (1962), and has become a popular methodology included in several econometrics textbook (e.g., Greene, 2003). To our knowledge, Anselin (1988) was the first author to discuss SUR from a spatial perspective. In his landmark text, Anselin discussed a model

made of "an equation for each time period, which is estimated for a cross section of spatial units" (p. 141). From this milestone, a large body of research has developed to extend the classical SUR into a spatial framework (e.g., Rey and Montouri, 1999; Lauridsen et al., 2010; Le Gallo and Dall'Erba, 2006; López et al., 2017).

The classical SUR model without spatial effects (from here, SUR-SIM) is a stack of equations as follows:

$$\begin{bmatrix} y_1 \\ y_2 \\ \vdots \\ y_T \end{bmatrix} = \begin{bmatrix} X_1 & 0 & \cdots & 0 \\ 0 & X_2 & \cdots & 0 \\ \vdots & \vdots & \ddots & \vdots \\ 0 & 0 & \cdots & X_T \end{bmatrix} \begin{bmatrix} \beta_1 \\ \beta_1 \\ \vdots \\ \beta_T \end{bmatrix} + \begin{bmatrix} \epsilon_1 \\ \epsilon_2 \\ \vdots \\ \epsilon_T \end{bmatrix} \tag{1}$$

where $y_t = (y_{1t}, ..., y_{Nt})$ is a $N \times 1$ vector, and in our case y_{st} is the incidence ratio in the province s $(s = 1, ..., N)$ the day t $(t = 1, ..., T)$; X_t is a $N \times k_t$ matrix of the k_t independent variables, with associated vector of coefficients β_t,; $\beta_t = (\beta_{1t}, ..., \beta_{Nt})$ is a vector of coefficients and $\epsilon_t = (\epsilon_{1t}, ..., \epsilon_{Nt})$ is the vector of residuals.

A key feature of the SUR model is the dependence structure among the vectors of residuals, namely:

$$E[\epsilon_t \epsilon'_{t'}] = \sigma_{tt'} \tag{2}$$

Note that this specification is very flexible, in that it allows changes in the coefficients β_{it} in order to modulate the effect of $X^i_{.t}$ on y_t. This flexibility can be reduced and it is posible to impose restrinctions considering some β coefficients as being constant over time. In this case, we can reformulate the coefficients expression $\beta_t = (\beta_1, \cdots, \beta_{r-1}, \beta_r, \beta_{r+1}, \cdots, \beta_{Nt})$ to restrict the first r coefficients to be constant across equations. This is equivalent to specifying some effects to be invariant over time.

Equation (1) can be rewriten in compact form:

$$\mathbf{Y} = \mathbf{X}\beta + \epsilon \tag{3}$$

where $\mathbf{Y}$ is now a vector of dimension $NT \times 1$, $\mathbf{X}$ is a block-diagonal matrix $NT \times K$ (with $K = \sum_t k_t$) and ϵ is an $NT \times 1$ vector. Using the Kronecker product notation ($\otimes$), the error matrix structure is expressed concisely as:

$$E[\epsilon\epsilon'] = \Sigma \otimes I_N; \ \Sigma = (\sigma_{tt'}) \tag{4}$$

As is the case with cross-sectional data, it is possible to test the residuals of Model (3) for spatial autocorrelation, and several tests have been developed to test the null hypothesis of spatial independence (see López et al., 2014). When the null hypothesis is rejected, several alternative specifications have been proposed to include spatial effects (Anselin, 1988, see also 2016). In this paper we consider a spatial SUR model that incorporates a spatial lag of the dependent variable as an explanatory factor. Spatial analytical approaches were used to

understand contagion-difussion processes in the case of infectious disease in general (e.g., Cliff et al., 1998) and the 2003-2004 SARS outbreak in particular (e.g., Meng et al., 2005; Cao et al., 2010). While we are mindful of the same caveat that the novel SARS-CoV2 may not follow the patterns of previous diseases, there is still evidence from the United States that COVID-19 displays spatial patterns that are consistent with a diffusion process (Desjardins et al., 2020). For this reason, the spatial lag model is appropriate to model incidence of COVID-19 geographically, since it accounts for potential spatial patterns that result from a process of contagion, as explained next.

The stack expresion for the SUR model with a spatially lagged dependent variable (SUR-SLM) is as follows:

$$\begin{aligned} \mathbf{AY} &= \mathbf{X}\beta + \epsilon \\ \epsilon &= N(0, \mathbf{\Sigma}) \end{aligned} \tag{5}$$

where $\mathbf{A} = \mathbf{I_{TN}} - \mathbf{\Gamma} \otimes \mathbf{W}$ is the spatially lagged dependent variable, and $\mathbf{\Gamma} = \mathbf{diag}(\rho_{\mathbf{1}}, \cdots, \rho_{\mathbf{T}})$.

This specification assumes that outcome (y_{st}) at location s and time t is partially determined by the weighted average (Wy_{st}) of the outcome in neighboring provinces, with neighborhood defined by matrix W of spatial weights. In other words, the spatially lagged dependent variable represents a process of contagion, where the disease in neighboring provinces can spillover in a spatial way. The coefficients of the spatially lagged variable are estimated for each time period ρ_t and identify the intensity and the sign of the contagion effect. It is possible test the null hypothesis of identical levels of spatial dependence ($\rho_i = \rho_j, \forall i, j$). The correspond Wald test is available in the `R` package `spsur`.

The SUR-SLM model can be estimated using maximum likelihood (López et al. (2014)) or instrumental variables (Mínguez et al. (2019)).

Analysis

Exploratory Data Analysis

Figure 1 shows the geographical variation in the incidence of COVID-19 in Spain, as well as the temporal progression of the disease in weekly averages. Our analysis begins on March 13, which is the first date when every province had reported at least one case of COVID-19. It can be seen that the highest incidence at this early date was in the provice of Álava, in the North of Spain. While not the most populous province, with a population of only 331,549, Álava has the highest GDP per capita of all provinces. Vitoria, its main city, is the capital of the Basque Country and has been the focus of efforts, along with San Sebastian and Bilbao, to develop a "Global Basque City" (Meijers et al., 2008). The other early focus of the pandemic in Spain was Madrid, which is the most populous province in the country and has the second highest GDP per capita after Álava. The early outbreaks in these two provinces can be traced throughout the progression of the pandemic over time, although by the end of the period under consideration, other provinces had matched and even surpased

their incidence rates, including Segovia and Soria to the north of Madrid, and Ciudad Real and Albacete to the south.

Figure 2 shows the distribution of the environmental variables in Spain. For ease of visualization we aggregate the provinces by Autonomous Community. Each box-and-whisker in the figure represents the distribution of the variable for a community over the 30-day period. In the plot, the communities have been sorted by latitude, so that Principado de Asturias is the northernmost community, and Canarias the southernmost. As seen in the figure, there is a relatively wide range of values both within and between provinces over the 30-day period examined. The top panel of the figure shows the distribution of mean temperatures. The lowest mean temperature for a community on any given day was 2.8C, and the highest 22.4C, for a range of approximately 20 degrees. Likewise, there is a great deal of variability in humidity, as seen in the middle panel of the figure, where the lowest mean humidity for any community is 48.3 and the highest is 99.6. Finally, the bottom panel displays mean daily hours of sunshine in the community. This variable displays the most variability within communities over time, but remains relatively constant across communities. It is important to note that these are summaries by community, and the actual values of these variables for the provinces display somewhat more variability.

Figure 3 includes three maps that display the spatial variation of our control variables, namely GDP per capita, percentage of older adults in province, population density, and presence of mass transit systems. As seen there, GDP per capita is higher in Madrid and the northeast part of the country, mainly in Pais Vasco and Cataluña. Percentage of older adults is somewhat more checkered, with high values in Madrid and other provinces in the center-west part of the country, but also in some provinces in the north. Outside of provinces with major cities (e.g., Madrid; Bizkaia and Gipuzkoa in Pais Vasco; Pontevedra in Galicia), population density tends to be higher in provinces along the Mediterranean coast. The final panel in the figure shows the five provinces in the country that have higher order mass transit systems (e.g., metro).

Figure 4 shows the distribution of daily simple correlations of incidence of COVID-19 with the independent variables (with the exception of Transit, which is a categorical variable). These correlations are calculated after log-transforming all variables. As previously discussed, the environmental variables have a temporal lag and were calculated different time windows.

It can be seen in the figure that temperature (in its three forms) has the highest simple correlation with incidence of COVID-19. After temperature, GDP per capita has the highest positive correlation with the dependent variable. The distribution of these correlations is also quite tight over the 30-day period of the study. Hours of sunshine tends to have a moderately high correlation with incidence of COVID-19, however the distribution of these correlations is more spread, and in some cases strays into negative values. A similar thing happens with humidity, which also tends to display more day to day variation in the correlation with the dependent variable. The percentage of older adults shows a relatively tight distribution of day-to-day correlations, and is negative. Population density, in contrast, tends to be negative, but is relatively spread, and

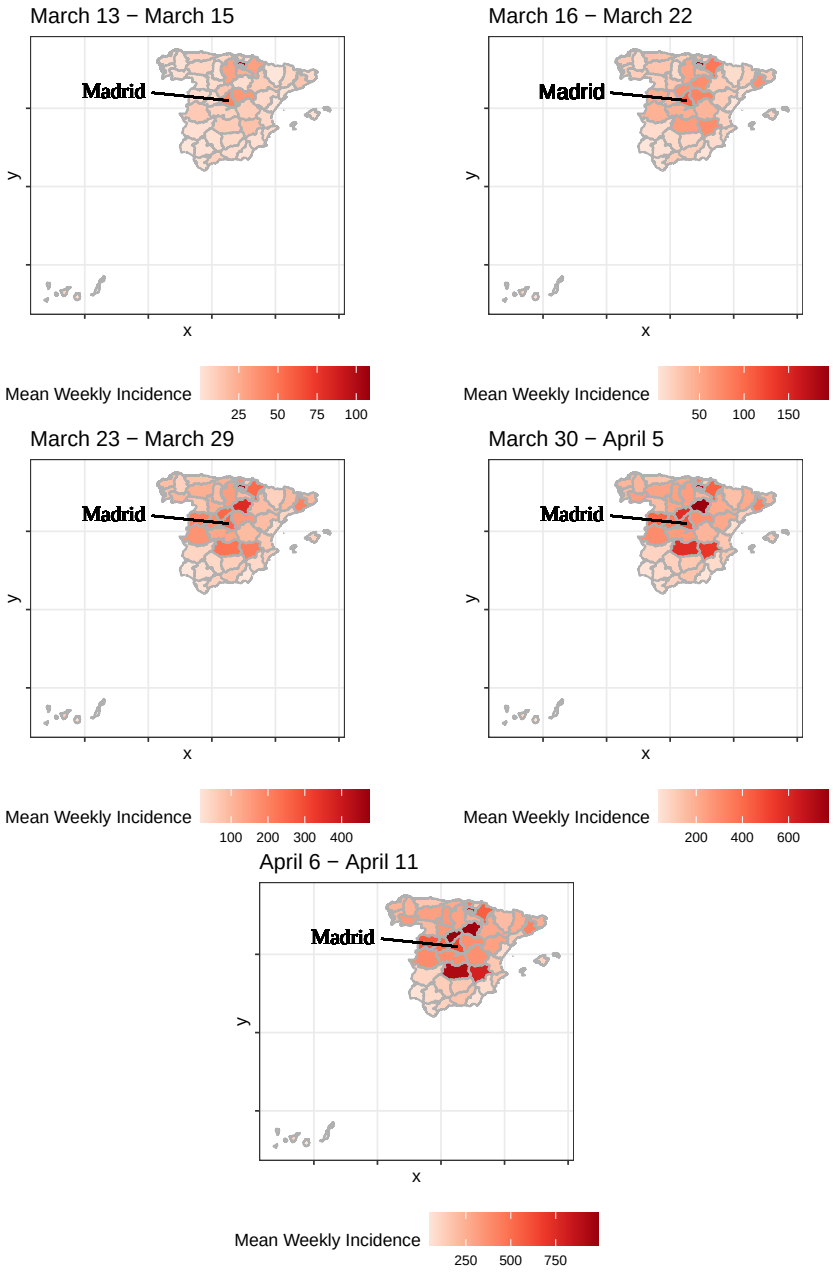

Figure 1: Mean weekly incidence of COVID-19 by province, in reported cases by 100,000 people

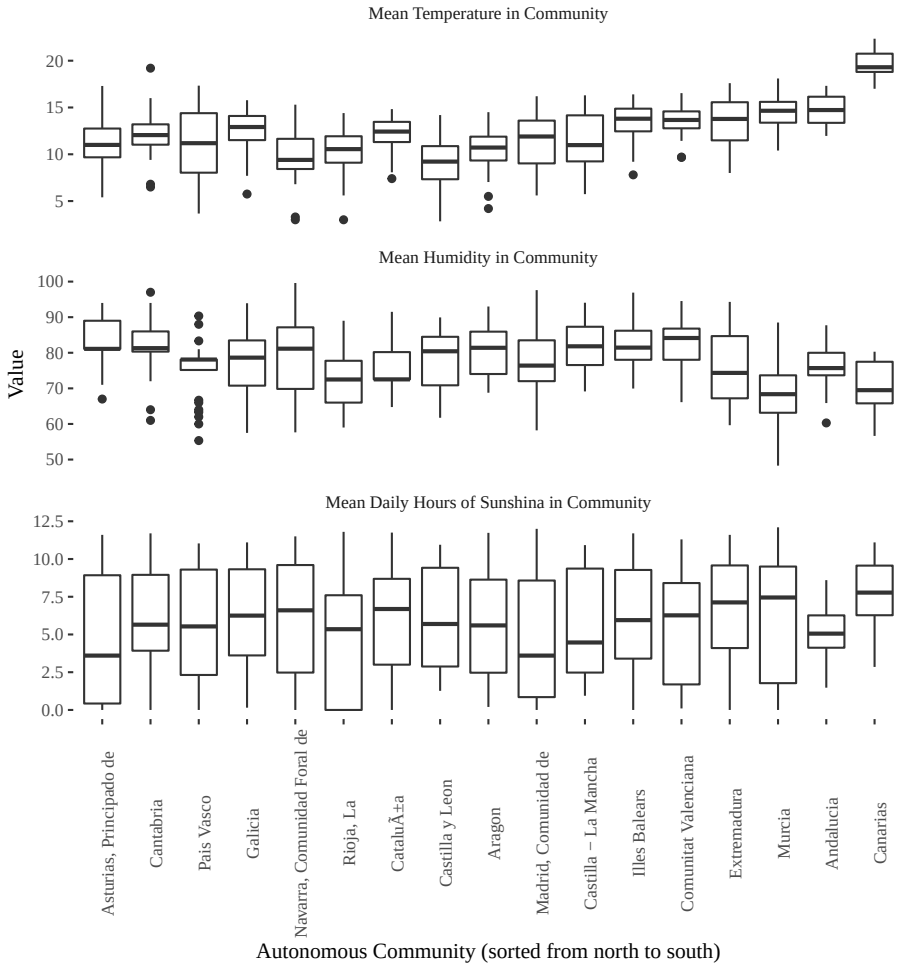

Figure 2: Distribution of mean temperatures and humidities in the Autonomous Communities in Spain between March 12, 2020 and April 11, 2020. The Autonomous Communities have been sorted by latitude, with communities to the left being the northermost, and to the right the southernmost

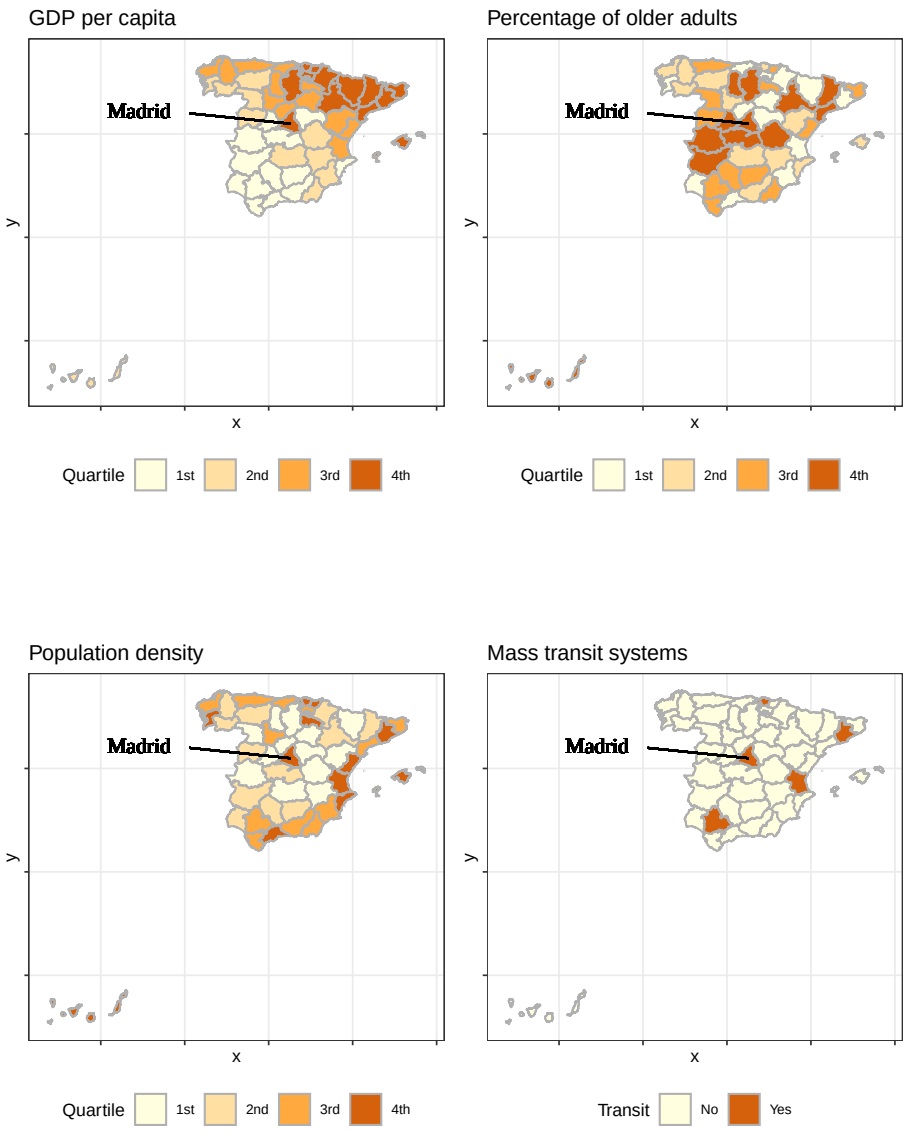

Figure 3: Spatial distribution of control variables by province

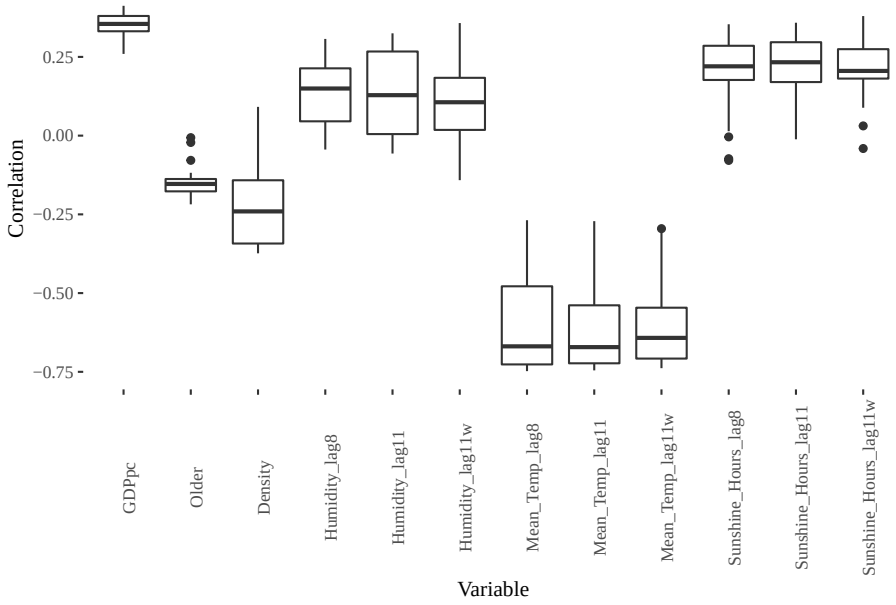

Figure 4: Distribution of daily correlations of the independent variables with daily incidence of COVID-19 (all variables have been log-transformed)

on some days, the simple correlation between density and incidence of COVID-19 is weakly positive.

SUR Models

Correlation analysis in the preceding section provides some insights about the potential associations between incidence of COVID-19 and the various environmental and control variables. In this section we estimate three spatial SUR models to test the differences between the various temporal lags and weighting schemes for the environmental variables. Accordingly, we define three models: Model 1, which is estimated using the lagged 8-day averages of the environmental variables (*lag8*); Model 2, which is estimated using the lagged 11-day averages of the environmental variables (*lag11*); and finally, Model 3, which is estimated using the lagged 11-day *weighted* averages of the environmental variables (*lag11w*).

To implement the SUR approach, we must define a matrix of spatial weights W. In this case, we consider neighborhoods based on adjacency, based on the well-known rook criterion (two provinces are adjacent if they share a boundary, but not if they touch only at a vertex). We modify this criterion in two cases. First, we make an allowance for adjacency between the two islands in the Autonomous Community of Canarias in the Pacific (Las Palmas and Santa Cruz de Tenerife),

which we assume are adjacent between each other. And secondly, we assume that Islas Baleares in the Mediterranean are adjacent to three provinces in Pais Catalans (i.e., Barcelona, Tarragona, and Castello). After matrix W has been specified, estimation of the model can proceed as usual.

For estimation, we log-transform the dependent and quantitative independent variables. The only variable that is not transformed is the categorical variable for transity systems. A log-log transformation is appropriate to capture non-linear relationships between variables and provides a straightforward interpretation of the coefficients as percentage change. Furthermore, we introduce restrictions so that the coefficients of two of our control variables are constant over time, namely GDP per capita and percentage of older adults. We do not see an *a priori* reason to let those two variables vary across equations, and the correlation analysis in Figure 4 also suggest little temporal variation. In contrast, we let the spatial autocorrelation parameter, as well as the parameters of the rest of the independent variables (including the constant) to vary over time[6].

After estimation, we compare the goodness of fit of the three SUR models. Figure 5 shows the equation-level coefficient of determination R^2, one for each time period/day. As well, the overall coefficient of determination for the system is reported for each model pooled $- R^2$. The general trend is identical for the three models, with the goodness-of-fit improving over time and plateuing around a value of R^2 of 0.6. Model 1 (*lag8*) performs somewhat better in the first few equations/days, when the goodness-of-fit is relatively poor, and then again in the last few equations/days. Model 3 (*lag11w*), in contrast, does not perform well towards the end of the study period. The most balanced model in terms of equation-level goodness-of-fit appears to be Model 1 (*lag11*), and this impression is further supported with a slightly higher value of the pooled $- R^2$. This analysis is in line with the incubation period reported by Lauer et al. (2020), although not the use of a weighted average. For the remainder of the paper, we will adopt Model 2 (*lag11*) as our best model. In the following section we discuss the results of the analysis in more depth.

Results and Discussion

Table 2 presents a summary.

Figure 6 shows the temporal evolution of the spatial autocorrelation coefficient (ρ) and the intercept of the model.

Figure 7 shows the temporal evolution of the coefficients for the two control variables that were not fixed over time, i.e., $\log(Density)$ and $Transit$.

Figure 8 shows the temporal evolution of the coefficient for the three environmental variables.

[6]We conducted sensitivity analysis letting all parameters vary over time, and while the results are qualitatively similar, the resulting models are less parsimonious. These results are available in the source R markdown document.

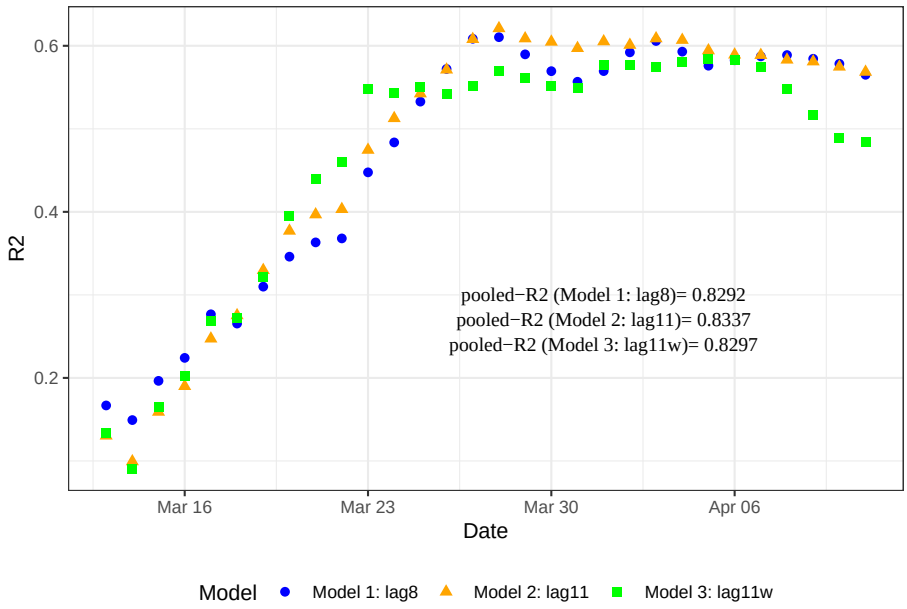

Figure 5: Goodness of fit of the SUR systems: by date and pooled

Table 2: Summary of estimation results of best model (lag11: lagged 11-day moving average)

	Estimates			Significance			
Variable	Min	Mean	Max	p > 0.10	0.10 <= p < 0.05	p <= 0.05	Note
Intercept	7.370	10.037	12.968	0	0	30	Non-constrained
log(GDPpc)	0.620	0.620	0.620	0	0	1	Constrained
log(Older)	-0.737	-0.737	-0.737	0	0	1	Constrained
log(Density)	-0.220	-0.097	0.153	19	0	11	Non-constrained
Transit	0.314	0.512	0.583	8	8	14	Non-constrained
log(Humidity)	-1.434	-0.534	-0.031	10	1	19	Non-constrained
log(Temperature)	-2.014	-1.406	-0.929	0	0	30	Non-constrained
log(Sunshine)	-0.258	0.097	0.206	7	2	21	Non-constrained
Spatially lagged y (rho)	0.015	0.142	0.528	12	3	15	Non-constrained

Note:
Significance: This is the number of coefficients with p-values as indicated
Non-constrained: coefficient was allowed to vary across equations
Constrained: coefficient as constant across equations

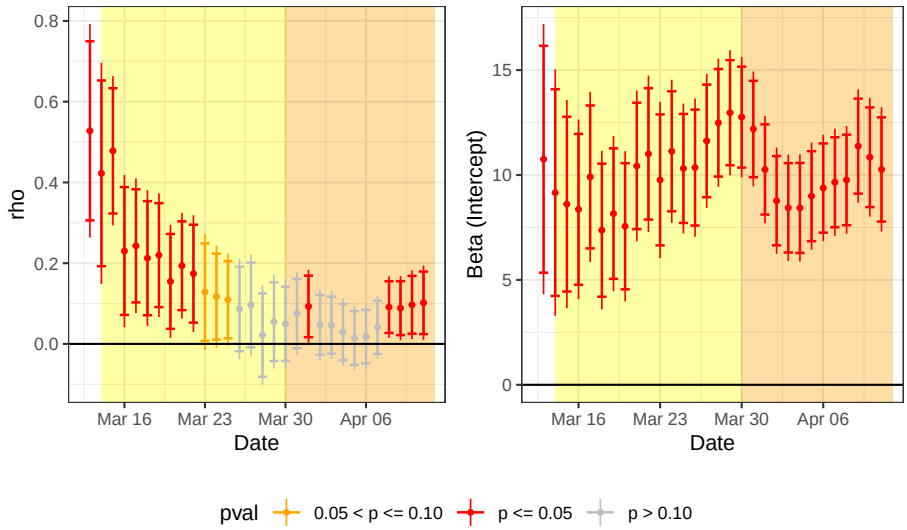

Figure 6: Temporal evolution of the spatial autocorrelation coefficient (rho) and the intercept of the model; dots are the point estimates and vertical lines are 95% confidence intervals. In yellow is the period after the declaration of the state of emergency, and in orange is the period when only essential activities were allowed.

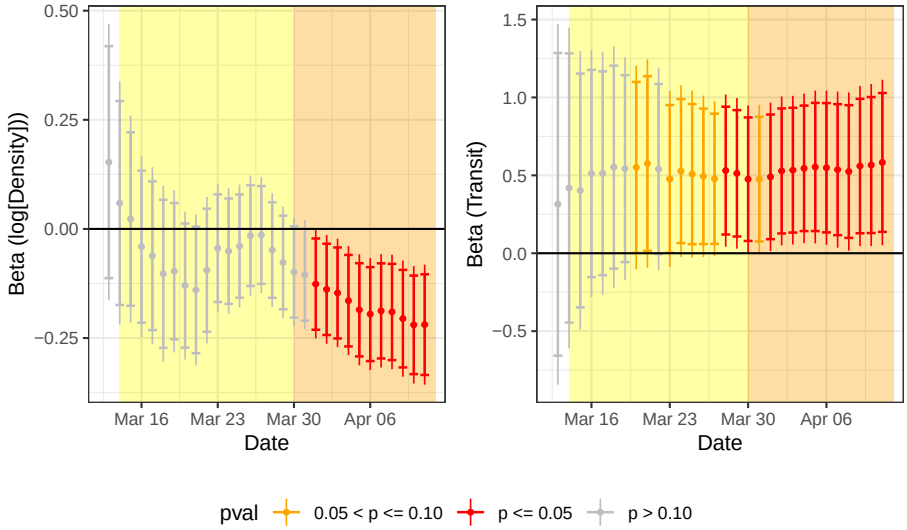

Figure 7: Temporal evolution of coefficient for the control variables; dots are the point estimates and vertical lines are 95% confidence intervals. In yellow is the period after the declaration of the state of emergency, and in orange is the period when only essential activities were allowed.

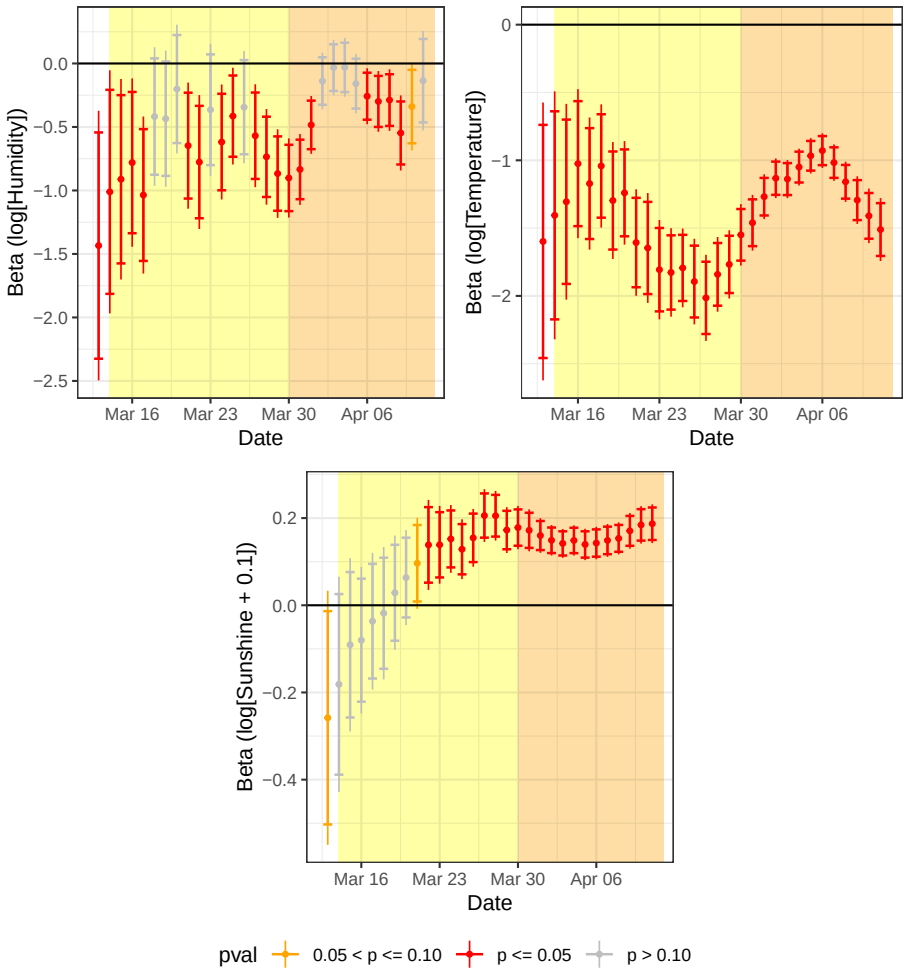

Figure 8: Temporal evolution of coefficient for the environmental variables; dots are the point estimates and vertical lines are 95% confidence intervals. In yellow is the period after the declaration of the state of emergency, and in orange is the period when only essential activities were allowed.

Concluding Remarks

More words go here.
Limitaciones

- La temperatura puedes ser un factor pero cabría esperar que no tuviera un impacto lineal. Por el contrario deberiamos esperar un 'punto de corte': Una temperatua mantenida superior a X grados durante siete días sea la mejor forma de incorporarla al modelo. En nuestro modelo (log-log) en incremento en un 1% de la temperatura se asocia con un incremento beta% en la incidencia. Esto es lo mismo si la temperatura es baja que si es alta.
- Idem para la humedad y horas de sol
- Los datos son 'provisionales'. Hay gran confusión sobre la incidencia real. La ausencia de test de diagnóstico PCRs al inicio de la pandemia (también ahora) puede desvirtuar el número de casos dianosticados.
- Los datos oficiales (que tampoco son fiables) son reportados a nivel de Comunidades Autónomas. La recopilación de datos a nivel de provincial son el resultado de un esfuerzo colaborativo de recopilacion entre distintas fuentes (principalmente gobiernos locales). Nuevamente puede haber sesgos importanes.
- En carácter insular de las Islas Canarias y de las Islas baleares no se ha tenido en cuenta.
- Baleares se ha linkado artificialmente con 3/4 provincias y debería de haberse dejado aislada para respetar su carácter insular al definir la matriz W.
- La incidencia depende de un estado inicial. Al inicio del estudio había provincias en las que la epidemia estaba muy desarrollada (Madrid/Alava) mientras que en otras apenas habías casos. Este hecho no ha sido considerado en el modelo. Decretar el confinamiento debe tener distintos impactos entre provincias. QUIZAR METER UNA VARAIBLE DUMMY CON COEF BETA CONSTANTE PARA CONTROLAR AQUELLAS PROVINCIAS CON MAYOR NUEMRO DE CASOS AL INICIO DEL CONFINAMIENTO.
- No se ha controlado por el sistema sanitario de cada provincia. Uno de los principales focos de contagio han sido los hospitales y los centros de salud. En aquellas provincias donde se ha promovido el mensaje "NO IR AL MEDICO" han presentado menor incidencia.
- ¿hasta que punto las variables de control no recojen también factores climáticos? por ejemplo, la gente jóven vive en el sur de España que ha tenido menos incidencia.

- Las estaciones meteorológicas para la obtencion de datos climáticos has sido elegidas aleatoriamente (una para cada provincia). otra seleccion puede dar otros resultados. AQUI SE PODRÍA HACER EL ESFUERZO DE CONSIDERARLAS TODAS (1000) Y CALCULAR LA MEDIA DE LAS VARAIBLES POR PROVINCIA

*IDEM para la humedad. idem para sunshine

- HACE FALTA INCLUIR UN PLOT CON LAS CORRELACIONES DE LOS RESIDUOS PARA DARLE RELEVANCIA A LA ESTIMACION SUR

Acknowledgments

Add acknowledgments as appropriate in final draft.

The following `R` packages were used in the course of this investigation and the authors wish to acknowledge their developers: `aemet` [], `ggthemes` (Arnold, 2019), `gridExtra` (Auguie, 2017), `kableExtra` (Zhu, 2019), `knitr` (Xie, 2015, 2014), `lubridate` (Grolemund and Wickham, 2011), `plm` (Millo, 2017), `rticles` (Allaire et al., 2020), `sf` (Pebesma, 2018), `spdep` (Bivand et al., 2013), spsur (Angulo et al., 2020) `tidyverse` (Wickham et al., 2019), `units` (Pebesma et al., 2016).

References

Allaire, J., Xie, Y., R Foundation, Wickham, H., Journal of Statistical Software, Vaidyanathan, R., Association for Computing Machinery, Boettiger, C., Elsevier, Broman, K., Mueller, K., Quast, B., Pruim, R., Marwick, B., Wickham, C., Keyes, O., Yu, M., Emaasit, D., Onkelinx, T., Gasparini, A., Desautels, M.-A., Leutnant, D., MDPI, Taylor and Francis, Ögreden, O., Hance, D., Nüst, D., Uvesten, P., Campitelli, E., Muschelli, J., Kamvar, Z.N., Ross, N., Cannoodt, R., Luguern, D., Kaplan, D.M., 2020. Rticles: Article formats for r markdown.

Angulo, A., Lopez, F.A., Minguez, R., Mur, J., 2020. Spsur: Spatial seemingly unrelated regression models.

Anselin, L., 1988. Spatial econometrics: Methods and models, Studies in operational regional science. Kluwer Academic Publishers, Dordrecht.

Anselin, L., 2016. Estimation and testing in the spatial seemingly unrelated regression (sur). Geoda Center for Geospatial Analysis; Computation, Arizona State University. Working Paper 2016-01.

Araujo, M.B., Naimi, B., 2020. Spread of sars-cov-2 coronavirus likely to be constrained by climate. medRxiv.

Arnold, J.B., 2019. Ggthemes: Extra themes, scales and geoms for 'ggplot2'.

Auguie, B., 2017. GridExtra: Miscellaneous functions for "grid" graphics.

Ángel Solá, D.E. de, Wang, L., Vázquez, M., Lázaro, P.A.M., 2020. Weathering the pandemic: How the caribbean basin can use viral and environmental patterns to predict, prepare and respond to covid-19. Journal of Medical Virology.

Bivand, R.S., Pebesma, E., Gomez-Rubio, V., 2013. Applied spatial data analysis with R, second edition. Springer, NY.

Cao, Z., Zeng, D., Zheng, X., Wang, Q., Wang, F., Wang, J., Wang, X., 2010. Spatio-temporal evolution of beijing 2003 sars epidemic. Science China Earth Sciences 53, 1017–1028. doi:10.1007/s11430-010-0043-x

Casanova, L.M., Jeon, S., Rutala, W.A., Weber, D.J., Sobsey, M.D., 2010. Effects of air temperature and relative humidity on coronavirus survival on surfaces. Appl. Environ. Microbiol. 76, 2712–2717.

Chan, K., Peiris, J., Lam, S., Poon, L., Yuen, K., Seto, W., 2011. The effects of temperature and relative humidity on the viability of the sars coronavirus. Advances in virology 2011.

Cliff, A., Haggett, P., Smallman-Raynor, M., 1998. Detecting space—time patterns in geocoded disease data. Cholera in london, 1854 measles in the united states, 1962–95, in: Geomed'97. Springer, pp. 13–42.

Coelho, M.T.P., Rodrigues, J.F.M., Medina, A.M., Scalco, P., Terribile, L.C., Vilela, B., Diniz-Filho, J.A.F., Dobrovolski, R., 2020. Exponential phase of covid19 expansion is not driven by climate at global scale. medRxiv.

Desjardins, M., Hohl, A., Delmelle, E., 2020. Rapid surveillance of covid-19 in the united states using a prospective space-time scan statistic: Detecting and evaluating emerging clusters. Applied Geography 102202.

Fernandes, N., 2020. Economic effects of coronavirus outbreak (covid-19) on the world economy. Available at SSRN 3557504.

Gong, B., Zhang, S., Yuan, L., Chen, K.Z., 2020. A balance act: Minimizing economic loss while controlling novel coronavirus pneumonia. Journal of Chinese Governance 1–20.

Greene, W.H., 2003. Econometric analysis. Pearson Education India.

Grolemund, G., Wickham, H., 2011. Dates and times made easy with lubridate. Journal of Statistical Software 40, 1–25.

Hallet, M., 2002. Regional specialisation and concentration in the eu, in: Regional Convergence in the European Union. Springer, pp. 53–76.

Harbert, R.S., Cunningham, S.W., Tessler, M., 2020. Spatial modeling cannot currently differentiate sars-cov-2 coronavirus and human distributions on the basis of climate in the united states. medRxiv.

Hu, H., Nigmatulina, K., Eckhoff, P., 2013. The scaling of contact rates with population density for the infectious disease models. Mathematical Biosciences 244, 125–134. doi:https://doi.org/10.1016/j.mbs.2013.04.013

Jaakkola, K., Saukkoriipi, A., Jokelainen, J., Juvonen, R., Kauppila, J., Vainio, O., Ziegler, T., Rönkkö, E., Jaakkola, J.J., Ikäheimo, T.M., 2014. Decline in temperature and humidity increases the occurrence of influenza in cold climate. Environmental Health 13, 22.

Jones, K.E., Patel, N.G., Levy, M.A., Storeygard, A., Balk, D., Gittleman, J.L., Daszak, P., 2008. Global trends in emerging infectious diseases. Nature 451, 990–993. doi:10.1038/nature06536

Kissler, S.M., Tedijanto, C., Goldstein, E., Grad, Y.H., Lipsitch, M., 2020. Projecting the transmission dynamics of sars-cov-2 through the postpandemic period. Science eabb5793. doi:10.1126/science.abb5793

Kudo, E., Song, E., Yockey, L.J., Rakib, T., Wong, P.W., Homer, R.J., Iwasaki, A., 2019. Low ambient humidity impairs barrier function and innate resistance against influenza infection. Proceedings of the National Academy of Sciences 116, 10905–10910.

Lancastle, N.M., 2020. Is the impact of social distancing on coronavirus growth rates effective across different settings? A non-parametric and local regression approach to test and compare the growth rate. medRxiv.

Lauer, S.A., Grantz, K.H., Bi, Q., Jones, F.K., Zheng, Q., Meredith, H.R., Azman, A.S., Reich, N.G., Lessler, J., 2020. The incubation period of coronavirus disease 2019 (covid-19) from publicly reported confirmed cases: Estimation and application. Annals of Internal Medicine. doi:10.7326/m20-0504

Lauridsen, J., Bech, M., López, F., Maté, M., 2010. A spatiotemporal analysis of public pharmaceutical expenditure. The Annals of Regional Science 44, 299–314.

Le Gallo, J., Dall'Erba, S., 2006. Evaluating the temporal and spatial heterogeneity of the european convergence process, 1980–1999. Journal of Regional Science 46, 269–288.

López, F.A., Martínez-Ortiz, P.J., Cegarra-Navarro, J.-G., 2017. Spatial spillovers in public expenditure on a municipal level in spain. The Annals of Regional Science 58, 39–65.

López, F.A., Mur, J., Angulo, A., 2014. Spatial model selection strategies in a sur framework. The case of regional productivity in eu. The Annals of Regional Science 53, 197–220.

Luo, S., Tsang, K.P., 2020. How much of china and world gdp has the coronavirus reduced? Available at SSRN 3543760.

Mäkainen, T.M., Juvonen, R., Jokelainen, J., Harju, T.H., Peitso, A., Bloigu, A., Silvennoinen-Kassinen, S., Leinonen, M., Hassi, J., 2009. Cold temperature and low humidity are associated with increased occurrence of respiratory tract infections. Respiratory medicine 103, 456–462.

Meijers, E., Hoekstra, J., Aguado, R., 2008. Strategic planning for city networks: The emergence of a basque global city? International Planning Studies 13, 239–259. doi:10.1080/13563470802521440

Meng, B., Wang, J., Liu, J., Wu, J., Zhong, E., 2005. Understanding the spatial diffusion process of severe acute respiratory syndrome in beijing. Public Health 119, 1080–1087. doi:https://doi.org/10.1016/j.puhe.2005.02.003

Millo, G., 2017. Robust standard error estimators for panel models: A unifying approach. Journal of Statistical Software 82, 1–27. doi:10.18637/jss.v082.i03

Mínguez, R., López, F., Mur, J., 2019. ML versus iv estimates of spatial sur models: Evidence from the case of airbnb in madrid urban area. The Annals of Regional Science 1–35.

Morency, C., Páez, A., Roorda, M.J., Mercado, R.G., Farber, S., 2011. Distance traveled in three canadian cities: Spatial analysis from the perspective of vulnerable population segments. Journal of Transport Geography 19, 39–50.

National Academies of Sciences, Engineering and Medicine, 2020. Rapid expert consultation on sars-cov-2 survival in relation to temperature and humidity and potential for seasonality for the covid-19 pandemic (april 7, 2020). The National Academies Press, Washington, DC. doi:doi:10.17226/25771

Pebesma, E., 2018. Simple Features for R: Standardized Support for Spatial Vector Data. The R Journal 10, 439–446. doi:10.32614/RJ-2018-009

Pebesma, E., Mailund, T., Hiebert, J., 2016. Measurement units in R. R Journal 8, 486–494. doi:10.32614/RJ-2016-061

Perez, L., Dragicevic, S., 2009. An agent-based approach for modeling dynamics of contagious disease spread. International journal of health geographics 8, 50.

Prem, K., Cook, A.R., Jit, M., 2017. Projecting social contact matrices in 152 countries using contact surveys and demographic data. PLoS computational biology 13, e1005697.

Rey, S.J., Montouri, B.D., 1999. US regional income convergence: A spatial econometric perspective. Regional studies 33, 143–156.

Roorda, M.J., Paez, A., Morency, C., Mercado, R., Farber, S., 2010. Trip generation of vulnerable populations in three canadian cities: A spatial ordered probit approach. Transportation 37, 525–548. doi:10.1007/s11116-010-9263-3

Sikder, S., Pinjari, A.R., 2012. Immobility levels and mobility preferences of the elderly in the united states evidence from 2009 national household travel survey. Transportation Research Record 137–147. doi:10.3141/2318-16

Singh, R., Adhikari, R., 2020. Age-structured impact of social distancing on the covid-19 epidemic in india. arXiv preprint arXiv:2003.12055.

The Novel Coronavirus Pneumonia Emergency Response Epidemiology Team, 2020. The epidemiological characteristics of an outbreak of 2019 novel coronavirus diseases (covid-19)—china, 2020. China CDC Weekly 2, 113–122.

Van Wagner, E., 2008. Toward a dialectical understanding of networked disease in the global city: Vulnerability, connectivity, topologies. Networked disease: Emerging infections in the global city 13–26.

Wang, J., Xiong, J., Yang, K., Peng, S., Xu, Q., 2010. Use of gis and agent-based modeling to simulate the spread of influenza, in: 2010 18th International Conference on Geoinformatics. IEEE, pp. 1–6.

Wickham, H., Averick, M., Bryan, J., Chang, W., McGowan, L.D., François, R., Grolemund, G., Hayes, A., Henry, L., Hester, J., Kuhn, M., Pedersen, T.L., Miller, E., Bache, S.M., Müller, K., Ooms, J., Robinson, D., Seidel, D.P., Spinu, V., Takahashi, K., Vaughan, D., Wilke, C., Woo, K., Yutani, H., 2019. Welcome to the tidyverse. Journal of Open Source Software 4, 1686. doi:10.21105/joss.01686

Xie, Y., 2014. Knitr: A comprehensive tool for reproducible research in R, in: Stodden, V., Leisch, F., Peng, R.D. (Eds.), Implementing Reproducible Computational Research. Chapman; Hall/CRC.

Xie, Y., 2015. Dynamic documents with R and knitr, 2nd ed. Chapman; Hall/CRC, Boca Raton, Florida.

Yao, Y., Pan, J., Liu, Z., Meng, X., Wang, W., Kan, H., Wang, W., 2020. No association of covid-19 transmission with temperature or uv radiation in chinese

cities. European Respiratory Journal 2000517. doi:10.1183/13993003.00517-2020

Zellner, A., 1962. An efficient method of estimating seemingly unrelated regressions and tests for aggregation bias. Journal of the American statistical Association 57, 348–368.

Zhou, Y.R., Coleman, W.D., 2016. Accelerated contagion and response: Understanding the relationships among globalization, time, and disease. Globalizations 13, 285–299.

Zhu, H., 2019. KableExtra: Construct complex table with 'kable' and pipe syntax.